Article

Seismic Design and Evaluation of Elevated Steel Tanks Supported by Concentric Braced Frames

Roberto Nascimbene [1],* and Gian Andrea Rassati [2]

1   Department STS, IUSS–Scuola Universitaria Superiore, 27100 Pavia, Italy
2   Department of Civil and Architectural Engineering and Construction Management, University of Cincinnati, Cincinnati, OH 45221, USA; gian.rassati@uc.edu
*   Correspondence: roberto.nascimbene@iusspavia.it

Abstract: The current investigation delved into the seismic analysis, design intricacies, and assessment of the response of elevated steel containment tanks when supported by concentrically braced frames. The primary focus was placed on comprehending the behavior of the supporting structure, recognizing its heightened vulnerability to damage under horizontal excitation—insights gleaned from reconnaissance teams studying earthquake aftermaths worldwide. A specific case study unfolded featuring a steel concentrically braced frame as the supporting structure, aligning with prevalent industry norms. Throughout the entire process, spanning design phases, seismic vulnerability assessments, and response evaluations, special emphasis was placed on the internal fluid sloshing phenomena. This nuanced consideration plays a pivotal role in shaping the dynamic response of the system. The study introduces two distinct design methods: the first method aligns with relevant international codes, while the second method innovatively incorporates the compressive strength of the braces into its approach. To evaluate the dynamic response of the elevated tank, both linear and nonlinear advanced analyses were employed. The comparative analysis of various strategies underscores the impact of the chosen design methodology on the overall system response. This multifaceted exploration aims to contribute valuable insights to the seismic resilience and design optimization of elevated steel containment tanks, furthering the understanding of their performance under seismic forces.

Keywords: steel structures; tanks; concentric braced frames; sloshing; silos

1. Introduction

Water storage tanks have played an indispensable role in modern societies since their inception. Among these critical structures, suspended tanks have found extensive applications in flat terrains and industrial facilities, with steel commonly employed for both the tanks and their support systems, especially in industrial contexts. However, in regions such as Italy and Europe, where seismic activity is a concern, a noticeable absence of specific regulations governing the design of these structures in high-seismicity areas has been observed [1]. The inherent irregularity in these structures, arising from the substantial mass of water at the top, combined with the intricate dynamic interplay between the fluid and the tank walls during horizontal accelerations (commonly referred to as sloshing), underscores the pressing need for specialized design criteria. In the absence of targeted regulations, addressing the seismic vulnerability of suspended tanks becomes imperative, necessitating a nuanced approach that accounts for the unique challenges posed by sloshing dynamics in high-seismicity regions. The operational resilience of elevated storage tanks following an earthquake holds paramount importance in sustaining water availability, especially for firefighting, which plays a critical role in mitigating extensive damage and preserving lives [2]. Additionally, in industrial tank facilities, the integration of measures to address natural–technological (Natech) events [3] is imperative for comprehensive risk management

and safety protocols. Natech events encompass natural calamities or hazardous incidents initiated by natural occurrences including earthquakes, floods, hurricanes, and tsunamis, which have the potential to trigger technological accidents.

Despite their critical role, past earthquakes have seen numerous elevated tanks sustaining varying degrees of damage, encompassing steel structures as well as reinforced concrete and precast materials, with the majority of issues linked to the supporting structure [4,5] (Figure 1). The historical instances of damage include the Kern County, California earthquake of 21 July 1952 (Figure 1a), the Chile earthquake of 22 May 1960 [6,7] (Figure 1b–d), the El Asnam, Algeria earthquake of 10 October 1980 (Figure 1e), the Bihar-Nepal earthquake of 21 August 1988 [4,8], the Jabalpur earthquake in the Indian state of Madhya Pradesh on 22 May 1997 [8], the Bhuj earthquake in the state of Gujarat, India, on 26 January 2001 [4,9–11] (Figure 1), the Maule earthquake of 27 February 2010 [12], and the Van earthquake in Turkey on 23 October 2011 [13]. This varied performance underscores the complex behavior attributed to the presence of two primary components: the tank containing the liquid and its supporting structure. While some elevated tanks have suffered damage in past earthquakes, it is noteworthy that this damage was predominantly localized in the supporting structures.

(**a**) (**b**) (**c**)

(**d**) (**e**) (**f**)

Figure 1. During earthquake events, a diverse array of configurations of elevated tanks sustain damage, illustrating the vast spectrum of vulnerabilities within these structures when subjected to seismic forces: (**a–d**) frame supports; (**e,f**) pile supports.

The intricate nature of these complexities poses significant challenges in the domains of structural design and modeling, making them a particularly captivating subject within the realm of structural analysis. In the field of civil engineering applications, there is a diverse array of configurations for elevated tanks, providing versatility and adaptability to cater to different requirements. These configurations can broadly be classified into three primary categories: frame elevated tanks, axisymmetrical pedestal elevated tanks, and composite elevated tanks. Numerous studies have been conducted to develop simplified procedures for a straightforward estimation of the seismic hazard associated with elevated tanks [5,14–23]. However, many of these studies often reference three main idealized models, each hinging on the specific simplifications adopted:

1. Single lumped-mass model in which the elevated tank has to be analyzed as a single degree of freedom system;
2. Two-mass uncoupled model in which two masses are assumed to be uncoupled and the earthquake forces on the support are estimated by considering two separate single degree of freedom systems;
3. Two-mass coupled model, in which the dynamic interaction between the two masses is explicitly taken into account using a spring model able to include the relation between the two masses.

The rationale behind the approach proposed in this research stems from the drawbacks associated with existing methods, particularly their simplifications. The single lumped-mass model, as suggested by Chandrasekaran and Krishna in [14], is reflected in seismic codes such as the Indian standard IS:1893 Clause 5.2 on "Elevated Tower-Supported Tanks" [9,24,25], ACI 371R-98 in Clause 4.7.5.2, ACI 371R-08 in Clause A5.1.2.8.2.1.5 (for concrete towers), and AWWA D100-11 Clause 13.4 (for steel towers). These codes permit the analysis of elevated tanks as a single degree of freedom system. Additionally, ASCE 7 in Clause 15.7.10.2 assumes that the material stored should be considered as a single rigid mass acting at the volumetric center of gravity. However, this approach is only effective for closed tanks fully filled with water (preventing vertical motion of water sloshing) or completely empty [5,26]. It is important to note that this assumption is realistic for long and slender tank containers with a height-to-radius ratio (H/R) ≥ 4 (Clause 14.4.7.5.1 FEMA 450). In such cases, all fluid mass participates in the impulsive mode of vibration, moving with the container wall in an impulsive fashion [3,9]. A more satisfactory alternative to the single-mass lumped model is the two-mass model proposed by Housner in [27], incorporated in Clause C3.11 NZSEE-09, Clause A.6 EC8-4, and Clause 4.2.2.4 IITK-GSDMA 2007 [28,29]. However, a drawback of this approach is that it assumes the two masses to be uncoupled, estimating earthquake forces on the support by treating them as two separate single-degree-of-freedom systems. The third method, proposed in [30], attempts to enhance the second method by coupling the masses. However, it lacks considerations for the supporting structures, a crucial aspect in earthquake capacity design.

Considering the limitations identified in the three methodologies previously examined, this paper introduces two distinct design approaches, namely one based on the Eurocode and the other representing the methodology proposed within this research. The first approach adheres closely to relevant international codes and standards, emphasizing conformity with established norms. In contrast, the second method introduces an innovative perspective by incorporating the compressive strength of the structural braces, presenting a unique and unconventional approach to design. To comprehensively evaluate the dynamic behavior of the elevated tank, an extensive array of analyses has been employed, encompassing both linear and nonlinear advanced techniques. The application of these analytical strategies has facilitated a comparative examination, offering insights into the substantial influence of the design process on the overall response of the entire system.

To enhance clarity regarding the flowchart of analyses involved in optimizing the design of an elevated steel tank and to facilitate a comprehensive understanding of the behavior of such a complex structure, the following steps are involved. The procedure,

which can be implemented and is fully reproducible using different applications and software from those used in this research, can be subdivided into the following steps:

Step 1: Design reference structures (or utilize a real case scenario). In this research, a simplified approach was employed for the pre-design of elevated tanks based on Malhotra's approach, as applied and described below;

Step 2: Calculate the main quantities involved in the procedure using Malhotra's approach including slenderness $\frac{H}{R}$, impulsive and convective masses (m_i, m_c), impulsive and convective heights (h_i, h_c) and seismic input as spectra and accelerograms, period of vibrations, and bending and shear forces;

Step 3: Moving from the quantities evaluated in the previous Step 2, determine the effects of applying a dynamic analysis to the elevated tanks using a linear modal response spectra analysis. The, compare this approach, considering diagonal compression, with the Eurocode 8 approach;

Step 4: In the real case scenario of earthquake engineering, the nonlinear approach is crucial. Therefore, apply a pushover analysis to the elevated tank cases to assess the dissipative capabilities of the designed structures;

Step 5: Compare the results obtained from Step 2 to Step 4, encompassing the simplified Malhotra's approach, linear spectra analysis, Eurocode 8 formulation, and verification with a nonlinear approach. Emphasize the effects brought about by the proposed approach, particularly considering diagonal compression.

2. Preliminary Assessment of Reference Structures

To illustrate the inherent complexities in designing and modeling such structures, a case study was undertaken on an elevated tank (Figure 2a), derived from a real-life example, as depicted in Figure 1a. This cylindrical tank was designed to hold a significant water mass of 226 tons within an 8 m diameter space, filled to a depth of 4.5 m. The steel walls, 10 mm thick, provided the required strength and structural integrity. The supporting structure for this tank was a concentrically braced frame (CBF) standing at an overall height of 18 m. This support structure comprised four columns placed at the vertices of a square with sides measuring 6 m. What distinguishes this study from others was the consideration of three distinct bracing configurations for the support structure, varying in the number of storeys from two to four (Figure 2). The utilization of CBFs in steel elevated tanks provides numerous significant advantages, as outlined in various research studies [31,32]. This informed the decision to choose CBFs as a case study, driven by their widespread adoption worldwide. These advantages include enhanced structural stability, minimized lateral deflections, optimized load distribution, cost-effectiveness, design flexibility, and alignment with industry standards.
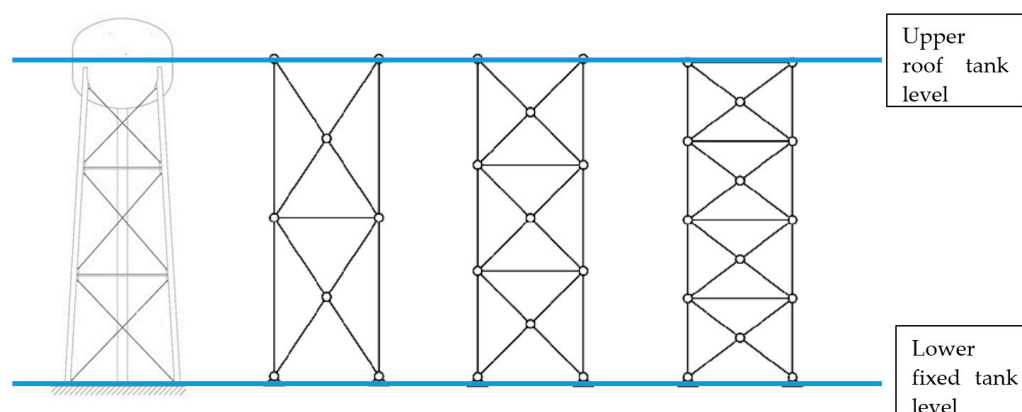

Figure 2. A depiction of a real elevated steel tank utilizing concentrically braced frames as supporting structures, along with illustrations showcasing three distinct configurations of the bracing for the support system.

The angle of inclination of the braces (β) relative to the horizontal axis is a crucial factor influencing the behavior of this structural system, as documented by Englekirk in [33]. Braced frames with a narrow base, like the 2-storey configuration, deform similarly to a cantilever system. On the other hand, frames with multiple tiers of braces at a shallower angle exhibit behavior more akin to that of a shear-type structure. The primary objective of this study was to determine the optimal X-bracing configuration for the design of suspended tanks, considering the intricate interplay of factors affecting their structural behavior.

Each of the three configurations considered in this study was customized to accommodate three distinct levels of seismic activity, resulting in the need to design a total of nine structures. These structures were designed to withstand varying levels of peak ground acceleration, with specific values set at 0.255 g, 0.188 g, and 0.07 g. This comprehensive approach allowed for a thorough exploration of structural responses under different seismic conditions.

In the seismic design of suspended tanks, a critical consideration is the accurate modeling of the dynamic interaction between the fluid inside the tank and the tank walls. Horizontal accelerations induce distinctive behaviors: the fluid near the surface tends to move vertically, creating convective waves characterized by a longer vibration period. In contrast, the lower part of the fluid translates rigidly with the tank itself (impulsive component). To effectively represent the sloshing phenomenon, many regulatory codes mandate the adoption of an equivalent mechanical model using two masses: convective and impulsive, as just described. Following this well-established approach, the model divides the mass of the water into two components: an impulsive mass and a convective mass. The impulsive mass refers to the portion of mass that moves synchronously with the tank wall, while the convective mass represents the upper level of fluid sloshing atop the reservoir. Both these components contribute to shear and bending moments at the base of the wall, exerting forces on the supporting structure.

For preliminary design purposes, a simplified approach allows for the estimation of the amplitudes of these two masses, as specified in EN 1998-4:2006 [34]. This method, originally developed by Malhotra in [35], provides a means to calculate the vibration periods for both the impulsive (T_{imp}) and convective (T_{conv}) components, offering valuable insights into the dynamic behavior of the tank under seismic conditions:

$$T_{imp} = C_i \frac{\sqrt{\rho}H}{\sqrt{s/R}\sqrt{E}} \tag{1}$$

$$T_{conv} = C_c \sqrt{R} \tag{2}$$

Here, the symbols represent the following parameters: ρ is the mass density of the liquid, H is the height of the free surface of the liquid, R is the tank radius, s is the thickness of the tank wall, and E is the modulus of elasticity of the tank material; the coefficients C_i and C_c are derived from Table 1; the coefficient C_i is dimensionless while C_c is in sec·m$^{-1/2}$.

Table 1. Coefficients C_i and C_c, impulsive and convective, used for the Malhotra procedure adopted at Point A.3.2.2 in EC8-4.

Malhotra	$\frac{H}{R} = 0.3$	$\frac{H}{R} = 0.5$	$\frac{H}{R} = 0.7$	$\frac{H}{R} = 1.0$	$\frac{H}{R} = 1.5$	$\frac{H}{R} = 0.7$	$\frac{H}{R} = 1.0$	$\frac{H}{R} = 1.5$
C_i	9.28	7.74	6.97	6.36	6.06	6.21	6.56	7.03
C_c	2.09	1.74	1.60	1.52	1.48	1.48	1.48	1.48

The shear force, denoted as V_b, and the overturning moment, denoted as M_b, at the base of the tank can be calculated based on the elastic response spectrum using the equations below:

$$V_b = (m_i + m_w + m_r)S_e(T_{imp}) + m_c S_e(T_{conv}) \tag{3}$$

$$M_b = (m_i h_i + m_w h_w + m_r h_r)S_e(T_{imp}) + m_c h_c S_e(T_{conv}) \tag{4}$$

In the given equations: m_i and m_c represent the impulsive and convective masses, respectively, m_w is the mass of the tank wall, and m_r is the mass of the tank roof, h_i and h_c are the heights from the base of the point of application of the resultant of the impulsive and convective hydrodynamic wall pressure, respectively, and h_w and h_r are the heights of the centers of gravity of the tank wall and roof, respectively. It is essential to note that the computation of internal actions considers the elastic spectral ordinate, S_e, as no hysteretic dissipation is expected within the system. While a more precise estimation of internal actions would involve factoring in the stiffness of the supporting structure, this would require prior knowledge of element sizes, leading to iterative design processes. For additional context, Table 2 offers an overview of the principal model properties for the examined tank.

Table 2. Overview of the primary parameters considered in the analysis employing the mechanical analogy approach.

m_i [ton]	m_c [ton]	h_i [m]	h_c [m]	T_{imp} [s]	T_{conv} [s]
131	95	1.93	2.82	0.035	3.010

The initial design of the supporting frames was carried out utilizing the calculated shear and overturning moment values at the tank base as per Equations (3) and (4) (refer to Table 3).

Table 3. Initial design values for the base shears and overturning moments of the fundamental case study structure.

PGA [g]	V_b [kN]	M_b [kNm]
0.255	1142	3671
0.188	966	3079
0.070	379	1198

In the design of CBFs, two distinct methods were employed: the approach specified in EN 1998-1:2004 [36], and an alternative method that accounts for the contribution of bracing elements under compression. Extensive experimental evidence consistently demonstrates that when a bracing element reaches its yielding point under tension, the element under compression retains at least 30% of its strength [37–39].

Under the first method, seismic resistance relies solely on the diagonal bracing elements in tension, with no consideration for the contribution of the bracing elements in compression. Consequently, the design of beams, columns, and frame connections adheres to capacity design principles, disregarding the potential support provided by the bracing elements in compression. On the other hand, the alternative method factors in both bracing elements in tension and those in compression when resisting the shear forces at different levels of the structure. The shear strength of a braced panel is determined by considering the bracing element in tension at its yield point and the strength of the compressed bracing element at 30% of its buckling load. This approach offers a more comprehensive perspective on the structural behavior under seismic forces.

In the assessment of the buckling critical load, a practical approach was adopted in which the effective length of the braces was set at 0.45 times the overall length of the brace, denoted as *L*. This choice was made to consider the level of constraint the brace in tension provides in the out-of-plane directions as well as the impact of the stiffness of the connections between the brace and the frame. This approach to determining the effective length aligns with the findings of previous research such as [40], providing a simplified yet effective means of modeling the structural behavior. Table 4 shows the outcome of the preliminary design for the braces according to the two methods considered.

Table 4. Outcome of braces design: Eurocode 8 vs. the proposed method.

Design Method	Configuration	Size
EC8	2-storey	RHS 140 × 140 × 5.4
EC8	3-storey	RHS 120 × 120 × 5.0
EC8	4-storey	RHS 135 × 135 × 4.0
Proposed	2-storey	RHS 135 × 135 × 5.6
Proposed	3-storey	RHS 135 × 135 × 4.0
Proposed	4-storey	RHS 135 × 135 × 3.6

The proposed design methodology, described in the next sections, stems from extensive research conducted by both authors on studies continuously exploring the application of compression braces in steel structures, aligning with the philosophy of capacity design principles and the hierarchy of resistance. It is essential to note that the effectiveness of the proposed method relies on assumptions regarding the effective length of braces and the calculation of brace buckling loads. In this paper, the proposed method was compared with the following four approaches:

1. Malhotra's simplified approach, which is scientifically accredited in Eurocode 8 Part 4 as a design procedure and is considered a well-established method in the field.
2. Response spectrum linear analysis was employed to ensure that the proposed approach was consistent with the "vibrating period", as observed in refined finite element modeling.
3. Advanced nonlinear fiber method to ensure that extending our approach to nonlinearity maintains consistency and clarity.
4. The classical codified approach proposed by Eurocode 8 Part 4.

3. Linear Analysis Results

The initial assessment of the performance of the designed supporting structures involved conducting linear analyses. These analyses utilized a modal response spectrum analysis with a finite element model. The model incorporated the two masses approach described above, which is related to Malhotra's methodology [35]. This approach accounts for impulsive (first degree of freedom) and convective (second degree of freedom) masses associated with the two primary fluid movements in the containment structure. In this linear approach, seismic forces were represented by a reduced response spectrum, taking into account the dissipative capabilities inherent in concentrically braced frame structures. While EN 1998-4:2006 [34] primarily addresses the dissipation of vibration modes related to the support structure, it does not apply reduction factors to convective modes within the fluid-filled tank. It is crucial to highlight that damping ratios must be differentiated for sloshing modes due to the significantly lower viscous dissipation associated with fluid motion. For sloshing modes, a recommended damping ratio of 0.5% was utilized [1,34]. In the linear analysis, the force reduction factor adhered to the EN 1998-1:2004 specifications [36], considering high ductility class frames with concentric bracing and accounting for structural irregularities along the height of the structures. This led to the application of a behavior factor of q = 2.8 in the analysis. The design spectrum for the three designated sites was established based on differing period ranges, analogous to approaches used in seismic isolation applications. This method is deemed suitable, as the vibration frequencies associated with structural and fluid motions are distinctly separate, with the transition period assumed to be 0.8 times the convective wave period.

The vibration characteristics of the system and the forces exerted at the base of the supporting structures were assessed through modal response spectrum analysis. Figure 3 illustrates the ratios between the shear forces at the base of the supporting structure determined through linear analysis and the corresponding values derived from the preliminary design considerations. The observed values generally aligned well with the expected outcomes,

particularly in regions characterized by high seismic activity. However, it is worth noting that the estimation tended to be conservative, despite some differences observed in the periods of vibration for the impulsive mode, as evaluated by the two different methods (refer to Table 5 for details). It is important to highlight in Table 5 that the convective period, representing the sloshing motion of fluid within the tank, is influenced primarily by the geometry and fluid properties rather than the structure's height or the CBF configuration. The geometry of the tank and the properties of the fluid largely dictate the natural frequency of convective motion. Hence, irrespective of the number of storeys, the convective period tends to remain relatively constant.
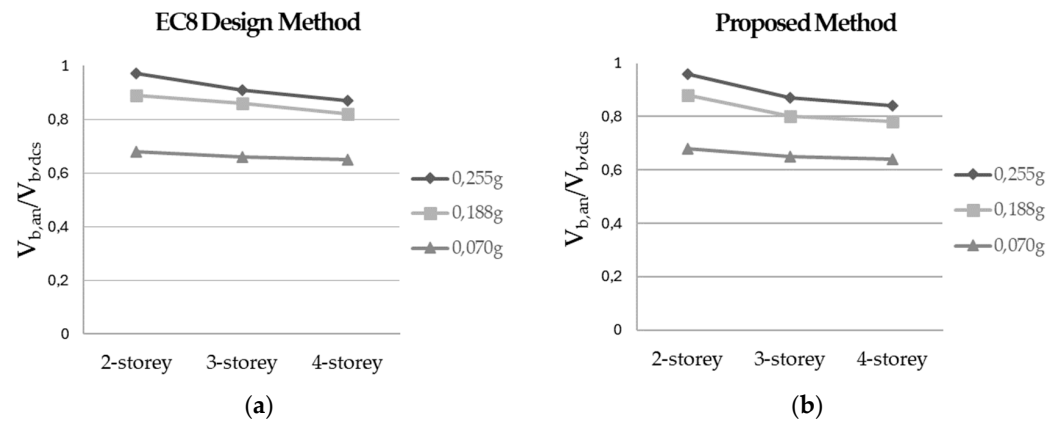

Figure 3. The dimensionless base shear values (Adapted from [41]) were derived after conducting simplified linear analyses using both the EC8 (**a**) design method and the proposed design method (**b**). This comparative assessment provides insights into the seismic response of the structure under different design approaches.

Table 5. The vibration periods resulting from the simplified linear analysis are as follows: impulsive mode (T_{imp}) in seconds and convective mode (T_{conv}) in seconds.

Design Method	Configuration	T_{imp} [s]	T_{conv} [s]
EC8	2-storey	0.44	3.02
EC8	3-storey	0.47	3.03
EC8	4-storey	0.51	3.03
Proposed	2-storey	0.45	3.02
Proposed	3-storey	0.50	3.03
Proposed	4-storey	0.54	3.03

The subsequent phase entailed constructing a linear finite element model using SAP2000 [42] for dynamic analyses via the modal response spectrum method (Figure 4a). Within this model, the containment structure was modeled using shell elements, while the structural elements of the support frame were represented using beam elements. To accurately simulate the dynamic interaction of the fluid inside the tank, two concentrated masses were integrated into the finite element models (refer to Figure 5). The first mass symbolized the impulsive component of the fluid and was rigidly linked to the containment structure. This mass was situated at the tank's center, positioned at a height denoted by h_i. Conversely, the second mass depicted the convective component of the fluid and was connected to the tank walls through a series of radial springs. This convective mass, located at height h_c, was linked to the tank walls through an array of radial springs engineered to maintain consistent stiffness across all diametric planes. This ensured that the structural response closely mirrored the desired behavior, as depicted in Figure 5. The masses and

their corresponding heights utilized in the modeling phase were established during the preliminary design, as outlined in Table 2. This ensured that the structural response closely mirrored the desired behavior, as depicted in Figure 5. The stiffness of each spring was meticulously finetuned to achieve uniform stiffness in the diametral direction, characterized as k_{c1}.
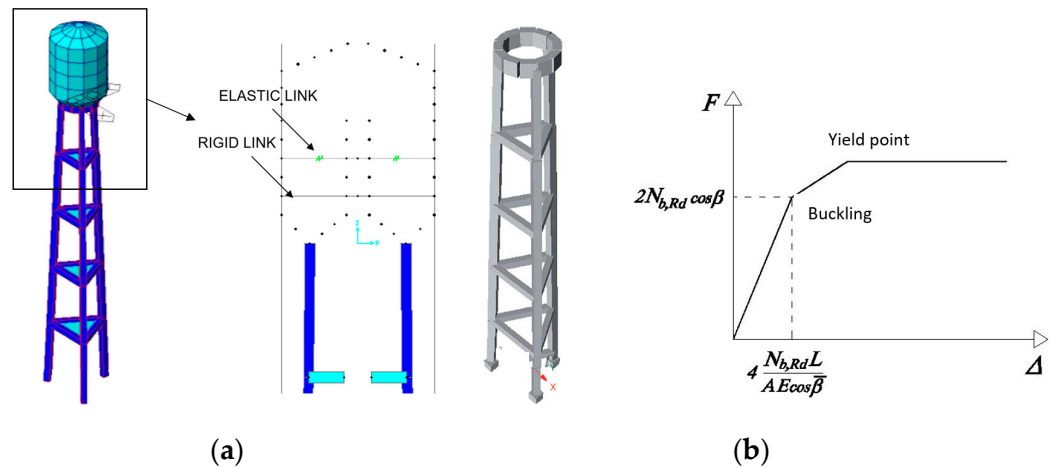

(**a**)   (**b**)

Figure 4. 3D models of a "reference" structure were developed solely for the purpose of visualizing the main geometry. In this modeling scheme, (**a**) the representation was implemented using SAP2000 software, where distinct masses were placed at impulsive and convective heights within the tank, connected via rigid and elastic links; and (**b**), a representative model was constructed using a fiber-based approach in Seismostruct, accompanied by a corresponding qualitative pushover curve.
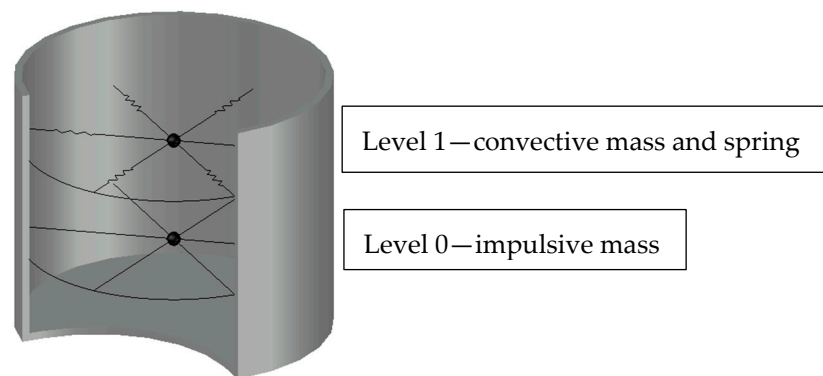

Figure 5. An equivalent mechanical model employing impulsive and convective elements was developed to simulate the fluid behavior within the structure. This modeling scheme was implemented using SAP2000 software, with distinct masses positioned at the impulsive and convective heights within the tank (as clearly represented in Figure 4a).

The finite element models utilized in the analysis provide a comprehensive depiction of both the supporting structure's stiffness and the dynamic interaction between the fluid and the containment structure (Figure 4a). Through the application of these analyses to different structural designs, it became evident that the preliminary design phase had significantly overestimated the magnitude of internal actions on the structural elements. This highlights the necessity of employing advanced modeling techniques to attain more accurate and dependable results in the design and analysis of such intricate systems.

Figure 6a illustrates the ratios between the maximum axial loads N_{Ed} observed on the first-storey columns and their respective strength N_{Rd}. The notable oversizing observed can be attributed to the simplicity of the model employed in the preliminary design of the frames as well as the influence of dissipation capabilities. These analyses incorporate the behavior factor, which was not accounted for during the design phase. Additionally,

Figure [6]b presents a comparison between the base shear values (V_b) assessed using different analysis methods (DES through the simplified approach, FEM using finite element model, and 2-DoF using the two degrees of freedom approximation indicated above) and the shear strength (V_{Rd}) provided by the diagonals arranged for the various configurations considered. The results validate the overestimation of the base shear demand with the simplified analysis. It is noteworthy that such a substantial degree of oversizing may lead to a structural response diverging from that anticipated through the utilization of a high behavior factor.
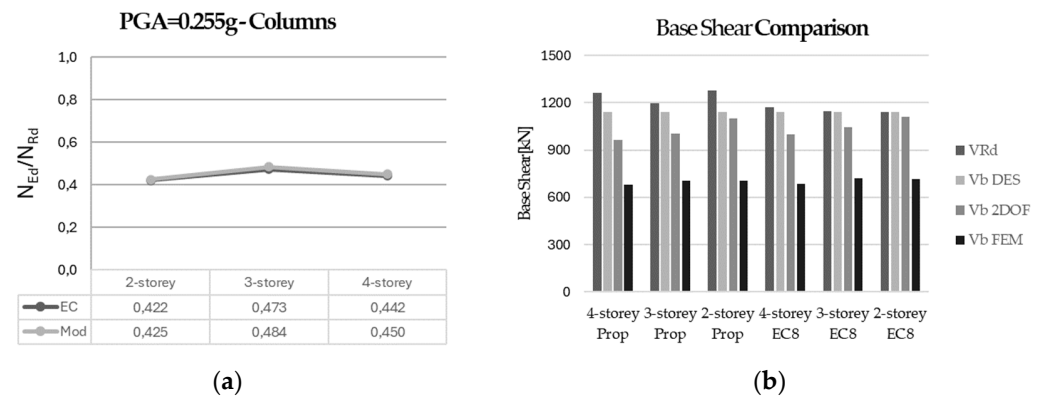

	2-storey	3-storey	4-storey
EC	0,422	0,473	0,442
Mod	0,425	0,484	0,450

(**a**)   (**b**)

Figure 6. Linear analysis results and comparisons (Adapted from [41]). (**a**) The dimensionless axial load on the column resulting from the finite element method (FEM) linear analysis. (**b**) A comparison of the base shear values evaluated through different analysis methods with the shear strength offered by the diagonals arranged for the various configurations under consideration.

4. Nonlinear Analysis Results

To comprehensively assess the dissipative capabilities of the designed structures, a series of nonlinear analyses were conducted, encompassing both static and dynamic assessments. A finite element model was developed, incorporating nonlinear properties in both material behavior and geometry. Notably, this model exclusively represents the support structure (Figure [4]b), while the fluid behavior is approximated using the lumped masses previously described, namely the impulsive and convective masses. To account for the buckling behavior of the bracing elements, an initial imperfection was introduced. The selection of the initial camber and the consideration of end restraint effects, as discussed in [43], are crucial aspects in the analysis of steel frames. Various approaches have been proposed in the scientific literature to address these factors:

1. In [44], an initial camber displacement ranging from 0.05% to 0.1% of the brace length is specified at the midspan of the brace;
2. In [45], the authors advocate for an initial camber of L/350, along with a sinusoidal deformed shape;
3. According to [46], a different approach is suggested, with an initial camber of L/1000 and a parabolic distribution.

These different approaches highlight the diversity of methods used to address the initial camber and end restraint effects in the analysis of steel frames. Each approach may have its own advantages and limitations, and the selection of the most appropriate method depends on various factors such as structural configuration, loading conditions, and designre quirements.

In our case, this imperfection involved an out-of-plane displacement at the midpoint of the elements, set at L/350, a method recommended in prior studies [44,45]. By employing this approach, a more precise evaluation of the structural response under nonlinear conditions including potential element buckling and other nonlinear effects could be achieved.

4.1. Pushover Analyses

Pushover analyses were conducted to evaluate the nonlinear behavior of the braces within the structure. Following the approach outlined in [47–49], these analyses utilized a lateral force distribution proportional to the first mode of vibration. The two lumped masses representing the fluid were rigidly connected to the supporting frame to simulate their effect. Figure 7 illustrates the axial force–deformation diagrams for a brace in tension and a brace in compression. These diagrams pertain to the supporting structure with three floors, originally designed using the method specified in [36] for the area of significant seismic activity under consideration. To aid comparison, the axial force values were normalized by dividing them by their respective design strengths in compression and tension. Notably, while the tensile strength was accurately predicted in the preliminary design process, the compressive strength, particularly in relation to buckling phenomena, was underestimated by approximately 30%. This discrepancy can be attributed to the effective length of the braces selected during the design phase. It is crucial to address this underestimation to prevent potential structural issues and ensure compliance with safety standards.
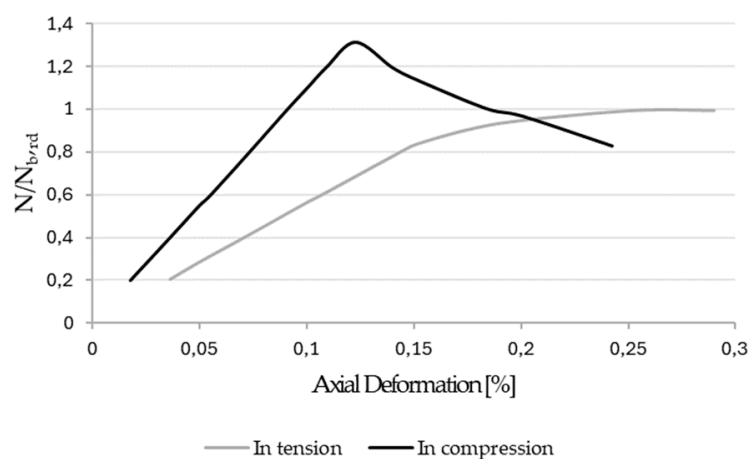

Figure 7. Dimensionless axial load versus deformation of braces (Adapted from [41]). In compression and in tension.

4.2. Time History Analyses

The finite element models initially developed for the nonlinear pushover analyses were further leveraged to conduct dynamic analyses, enabling a comprehensive exploration of the interaction between the fluid and the supporting structure. In these dynamic analyses, the impulsive mass remained rigidly connected to the containment structure, while the convective mass was linked through a system of elastic springs, consistent with the setup used in the linear analyses. A total of fifteen natural accelerograms were employed for these dynamic analyses, carefully selected to align with the elastic spectrum utilized during the design phase, specifically tailored to the region with the highest seismic activity (Table 6). Compatibility between these spectra and the recorded elastic spectra was rigorously assessed within a period range spanning from 0.15 to 2 s, ensuring adherence to the acceptable deviation limits as discussed in [50]. The dynamic analyses were conducted exclusively for the 3- and 4-floor configurations, designed according to both previously considered methods. The 2-floor solution was excluded due to its less efficient response to horizontal forces and limited material savings. Verification of individual structural elements was performed by comparing the average values of the maximum internal actions observed in each analysis with the corresponding design strengths. This verification process focused on the most stressed braces, beams, and columns on each floor, ensuring compliance with the necessary safety and performance criteria.

Table 6. Ground motion records: far field conditions; EC8 site conditions type C (180m/s < V_s30 < 360 m/s) and Magnitude ranging from 5.0 to 8.0.

Event	Year	$M_w//M_l//M_s$	Distance [km]	PGA [g]
Imperial Valley	1979	6.5//6.6//6.9	43.6 (Rrup)	0.351
Chi-Chi	1999	7.6//7.3//7.6	20.4 (Rrup)	0.294
Duzce	1999	7.1//7.2//7.3	17.6 (Rrup)	0.822
Livermore	1980	5.4//5.4//5.5	17.6 (Rrup)	0.301
Loma prieta	1989	6.9//-//7.1	16.1 (Rrup)	0.417
Northridge	1994	6.7//6.6//6.7	15.8 (Rrup)	0.356
S. Fernando	1971	6.6//-//6.6	21.2 (Rrup)	0.174
Kocaeli	1999	7.4//-//7.8	31.8 (Rrup)	0.136
Whittier Narrows	1987	6.0//5.9//5.7	16.9 (Rrup)	0.333
Friuli, 2nd shock	1976	5.6//-//5.8	19.5 (Repi)	0.233
Irpinia	1980	6.90//-//-	29.8 (Rrup)	0.145
Val Comino	1984	5.9//5.9//5.8	19.7 (Repi)	0.145
Umbria-Marche 1st shock	1997	5.7//5.6//5.6	24.5 (Repi)	0.101
Umbria-Marche 2st shock	1997	6.0//5.8//6.1	21.5 (Repi)	0.172
L'Aquila	2009	6.3//5.8//-	34.9 (Repi)	0.069

As depicted in Figure 8a, it was evident that the braces within the supporting structures experienced tensile stresses N_{Ed} well below their design strengths N_{Rd}. This indicates a conservative approach in the design process, where the structures were engineered with more strength in tension than necessary. In contrast, when assessing the maximum compressive axial loads (Figure 8b), it was noticeable that these loads surpassed what was considered during the preliminary design phase ($N_{b,Rd}$ is the buckling axial design resistance). These findings align with the results obtained in the nonlinear static analyses. Overall, the supporting structures exhibited predominantly linear behavior due to significant oversizing of their components. This oversizing can be attributed to a conservative assessment of earthquake-induced horizontal forces during the design phase.
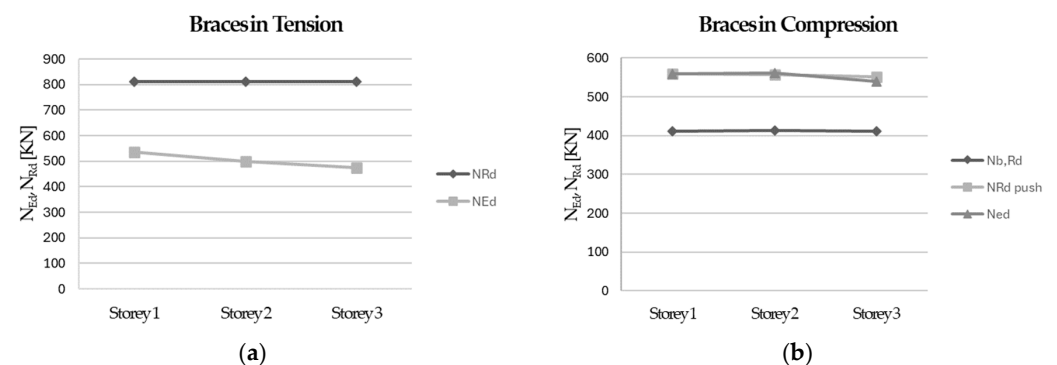

Figure 8. Internal actions of braces (Adapted from [41]): (**a**) compression, (**b**) tension.

Upon examining the internal actions in the columns (Figure 9), despite the considerable oversizing of the structure, these actions only slightly fell below the provided strength ($N_{b,Rd}$). According to the principles of capacity design, the initial underestimation of the compressive strength of the braces during the design phase led to a corresponding

underestimation of the axial loads (N_{Ed}), for which the columns needed to be dimensioned. This disparity becomes evident when comparing the expected axial force in columns with the observed values resulting from the nonlinear dynamic analysis, underscoring the importance of a more accurate estimation of brace compressive strength in the design process.
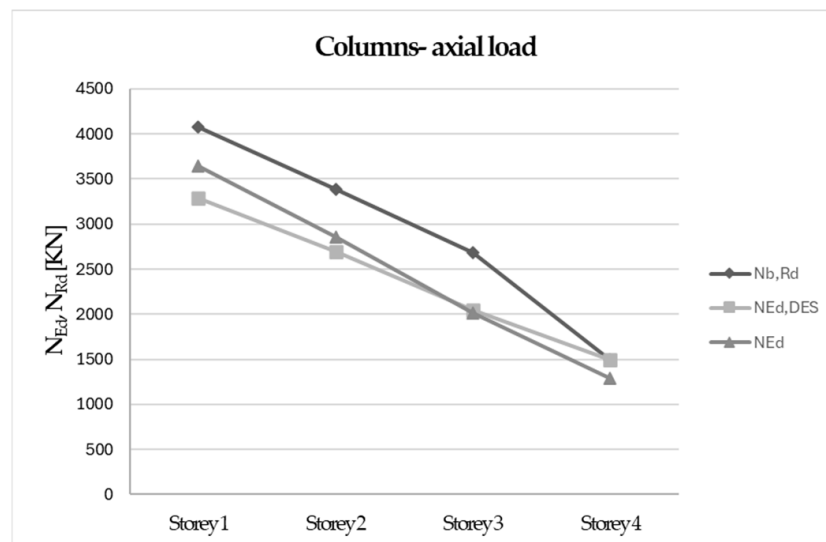

Figure 9. Internal actions in the columns (Adapted from [41]).

5. Conclusions and Recommendations

The structures investigated in this study exhibited a noticeable degree of oversizing, primarily stemming from an initial overestimation of earthquake-induced actions during the preliminary design phase of the tank supporting structures. This overestimation can be attributed to the reliance on highly simplified models, which tended to inflate the anticipated forces and stresses. However, upon conducting the linear finite element model analysis, a significant level of conservatism in the preliminary design was uncovered. This prompted a thorough reassessment and modification of section choices for various structural elements at that stage of the analysis.

Further insight into the behavior of the supporting structures was gleaned from the nonlinear analyses, revealing critical aspects overlooked by linear analysis alone. Specifically, nonlinear analyses provided a more nuanced and accurate depiction of brace buckling behavior, which is crucial for estimating the column internal actions. It became evident that the actions on the columns were more severe than initially anticipated from the linear analyses, highlighting the importance of considering the nonlinear effects in structural design assessments. The integration of compression braces into the performance evaluation of elevated frames, coupled with the consideration of fluid behavior, through the proposed methods, has yielded a powerful tool for designing robust and high-performing elevated tanks.

Structures designed using the proposed method demonstrated a response similar to that observed for concentrically braced frames designed according to [36], despite a notable 15% reduction in material usage. It is crucial to acknowledge that the effectiveness of this method relies on assumptions regarding the effective length of braces and the calculation of brace buckling loads.

Upon comparing various geometric configurations, storey braces, and seismic accelerograms as inputs for time history analysis, it became evident that solutions with 3- and 4-storeys exhibited superior lateral behavior and boasted lighter structures in comparison to the 2-storey configuration when evaluated against the proposed approach.

Several potential future developments and applications can be envisioned for this research:

1. Refinement of design methods: Further refinement and optimization of the proposed design methods to enhance efficiency and accuracy in designing elevated tanks.
2. Exploration of advanced modeling techniques: Investigation of advanced modeling techniques such as nonlinear explicit dynamic finite element analysis (ALE or SPH) to capture more intricate structural behaviors and improve the design accuracy.
3. Integration of new materials: Exploration of the integration of new materials such as advanced composites or high-strength alloys to further optimize the structural performance of elevated tanks.
4. Application to different contexts: Application of the developed design methodologies to different contexts such as other types of structures or in regions with different seismic and environmental conditions.
5. Development of decision support tools: Development of decision support tools or software packages based on the research findings to assist engineers and designers in efficiently and accurately designing elevated tanks.
6. Incorporation of sustainability principles: Integration of sustainability principles into the design process to minimize environmental impact and optimize resource utilization in the construction and operation of elevated tanks.
7. Additionally, efforts may focus on developing less conservative simplified models for the preliminary assessment of the seismic response of this structural system, thereby enhancing the efficiency and accuracy of the design process.

Author Contributions: Conceptualization, G.A.R.; Methodology, G.A.R. and R.N.; Software, R.N.; Validation, R.N.; Writing—original draft preparation, R.N.; Writing—review and editing, G.A.R.; Supervision, G.A.R. All authors have read and agreed to the published version of the manuscript.

Data Availability Statement: Data are contained within the article.

References

1. Calvi, G.M.; Nascimbene, R. *Seismic Design and Analysis of Tanks*, 1st ed.; Wiley: New York, NY, USA, 2023.
2. Livaoglu, R.; Dogangun, A. Simplified seismic analysis procedures for elevated tanks considering fluid-structure-soil interaction. *J. Fluids Struct.* **2006**, *22*, 421–439. [CrossRef]
3. Ricci, F.; Yang, M.; Reniers, G.; Cozzani, V. Emergency response in cascading scenarios triggered by natural events. *Reliab. Eng. Syst. Saf.* **2024**, *243*, 109820. [CrossRef]
4. Hirde, S.; Bajare, A.; Hedaoo, M. Seismic performance of elevated water tanks. *Int. J. Adv. Eng. Res. Stud.* **2011**, *1*, 78–87.
5. Moslemi, M. Seismic Response of Ground Cylindrical and Elevated Conical Reinforced Concrete Tanks. Ph.D. Thesis, Ryerson University, Toronto, ON, Canada, 2011.
6. Arze, E. Seismic failure and repair of an elevated water tank. In Proceedings of the 4th World Conference on Earthquake Engineering, Santiago, Chile, 13–18 January 1969; Volume III, pp. B6-57–B6-69.
7. Steinbrugge, K.V.; Flores, R.A. The chilean earthquakes of May, 1960: A structural engineering viewpoint. *Bull. Seismol. Soc. Am.* **1963**, *53*, 225–307. [CrossRef]
8. Jain, S.K.; Sameer, S.U. A review of requirements in indian codes for aseismic design of elevated water tanks. *Bridge Struct. Eng. IABSE* **1993**, *23*, 1–16.
9. Rai, D.C. Seismic retrofitting of R/C shaft support of elevated tanks. *Earthq. Spectra* **2002**, *18*, 745–760.
10. Rai, D.C. Review of code design forces for shaft supports of elevated water tanks. In Proceedings of the 12th Symposium on Earthquake Engineering, IIT Roorkee, India, 16–18 December 2002; pp. 1407–1418.
11. Rai, D.C. Performance of elevated tanks in Mw 7.7 Bhuj earthquake of January 26th, 2001. *J. Earth Syst. Sci.* **2003**, *112*, 421–429. [CrossRef]
12. Eidinger, J.M. Performance of water systems during the Maule Mw 8.8 earthquake of 27 February 2010. *Earthq Spectra* **2012**, *28*, S605S620. [CrossRef]
13. Uckan, E.; Akbas, B.; Shen, J.; Wen, R.; Turandar, K.; Erdik, M. Seismic performance of elevated steel silos during Van earthquake, October 23, 2011. *Nat. Hazards* **2015**, *75*, 265–287. [CrossRef]
14. Chandrasekaran, A.R.; Krishna, J. Water towers in seismic zones. In Proceedings of the 3rd World Conference on Earthquake Engineering, Auckland, New Zealand, 22 January–1 February 1965; Volume IV, pp. 161–171.

15. El Damatty, A.A.; Korol, R.M.; Mirza, F.A. Stability of elevated liquid-filled conical tanks under seismic loading. Part I—Theory. *Earthq. Eng. Struct. Dyn.* **1997**, *26*, 1191–1208. [CrossRef]

16. El Damatty, A.A.; Korol, R.M.; Mirza, F.A. Stability of elevated liquid-filled conical tanks under seismic loading. Part II—Applications. *Earthq. Eng. Struct. Dyn.* **1997**, *26*, 1209–1229. [CrossRef]

17. Garcia, S.M. Earthquake response analysis and aseismic design of cylindrical tanks. In Proceedings of the 4th World Conference on Earthquake Engineering, Santiago, Chile, 13–18 January 1969; Volume II, pp. B4-169–B4-182.

18. Haroun, M.A.; Ellaithy, H.M. Seismically induced fluid forces on elevated tanks. *J. Tech. Top. Civ. Engng* **1985**, *111*, 1–15. [CrossRef]

19. Ifrim, M.; Bratu, C. The effect of seismic action on the dynamic behavior of elevated water tanks. In Proceedings of the 4th World Conference on Earthquake Engineering, Santiago, Chile, 13–18 January 1969; Voume II, pp. B4-127–B4-142.

20. Moslemi, M.; Kianoush, M.R.; Pogorzelski, W. Seismic response of liquid filled elevated tanks. *Eng. Struct.* **2011**, *33*, 2074–2084. [CrossRef]

21. Ramiah, B.K.; Gupta, D.S.R.M. Factors effecting seismic design of water towers. *ASCE J. Struct. Div.* **1966**, *92*, 13–30. [CrossRef]

22. Shepherd, R. The two mass representation of a water tower structure. *J. Sound. Vib.* **1972**, *23*, 391–392, IN1, 393–396. [CrossRef]

23. Sweedan, A.M.I. Equivalent mechanical model for seismic forces in combined tanks subjected to vertical earthquake excitation. *Thin-Walled Struct.* **2009**, *47*, 942–952. [CrossRef]

24. Rai, D.C.; Singh, B. Seismic design of concrete pedestal supported tanks. In Proceedings of the 13th World Conference on Earthquake Engineering, Vancouver, BC, Canada, 1–6 August 2004; p. 230.

25. *IS 1893*; Recommendations for Earthquake Resistant Design of Structures. Bureau of Indian Standards: Old Delhi, India, 2016.

26. McLean, R.S.; Moore, W.W. Computation of the vibration period of steel tank towers. *Bull. Seismol. Soc. Am.* **1936**, *26*, 63–67. [CrossRef]

27. Housner, G.W. The dynamic behaviour of water tanks. *Bull. Seismol. Soc. Am.* **1963**, *53*, 381–387. [CrossRef]

28. Jain, S.K.; Jaiswal, O.R. Modified proposed provisions for aseismic design of liquid storage tanks: Part I—Codal provisions. *ASCE J. Struct. Eng.* **2005**, *32*, 195–206.

29. Jain, S.K.; Jaiswal, O.R. Modified proposed provisions for aseismic design of liquid storage tanks: Part II—commentary and examples. *ASCE J. Struct. Eng.* **2005**, *32*, 297–310.

30. United States Atomic Energy Commission titled "Nuclear Reactors and Earthquake," Reactor technology TID-4500 (22nd Edition, August 1963, TID-7024). Available online: https://digital.library.unt.edu/ark:/67531/metadc1030393/m2/1/high_res_d/4620608.pdf (accessed on 12 February 2024).

31. Rodríguez, D.; Brunesi, E.; Nascimbene, R. Fragility and sensitivity analysis of steel frames with bolted-angle connections under progressive collapse. *Eng. Struct.* **2021**, *2281*, 111508. [CrossRef]

32. Wijesundara, K.K.; Nascimbene, R.; Rassati, G.A. Evaluation of the seismic performance of suspended zipper column concentrically braced steel frames. *J. Constr. Steel Res.* **2018**, *150*, 452–461. [CrossRef]

33. Englekirk, R. *Steel Structures—Controlling Behaviour through Design*; John Wiley & Sons Inc.: Hoboken, NJ, USA, 1994.

34. *EN 1998-4:2006*; Eurocode 8: Design of Structures for Earthquake Resistance—Part 4: Silos, Tanks and Pipelines. CEN: Brussels, Belgium, 2006.

35. Malhotra, P.K. Practical nonlinear seismic analysis of tanks. *Earthq. Spectra* **2000**, *16*, 473–492. [CrossRef]

36. *EN 1998-1:2004*; Eurocode 8: Design of Structures for Earthquake Resistance—Part 1: General Rules, Seismic Actions and Rules for Buildings. CEN: Brussels, Belgium, 2004.

37. Black, R.G.; Wenger, W.A.; Popov, E.P. Inelastic Buckling of Steel Struts under Cyclic Load Reversal. Berkeley Earthquake Engineering Research Center, University of California. 1980. Available online: https://nehrpsearch.nist.gov/static/files/NSF/PB81154312.pdf (accessed on 15 February 2024).

38. Tremblay, R. Inelastic seismic response of steel bracing members. *J. Constr. Steel Res.* **2002**, *58*, 665–701. [CrossRef]

39. Tremblay, R.; Archambault, M.H.; Filiatrault, A. Seismic response of concentrically braced steel frames made with rectangular hollow bracing members. *J. Struct. Eng.* **2003**, *129*, 1626–1636. [CrossRef]

40. Nascimbene, R.; Rassati, G.A.; Wijesundara, K.K. Numerical simulation of gusset plate connections with rectangular hollow section shape brace under quasi-static cyclic loading. *J. Constr. Steel. Res.* **2012**, *70*, 177–189. [CrossRef]

41. Fagà, E.; Rassati, G.A.; Nascimbene, R. Seismic Design of Elevated Steel Tanks with Concentrically Braced Supporting Frames. In Proceedings of the Structures Congress 2012, Chicago, IL, USA, 29–31 March 2012; American Society of Civil Engineers: Reston, VA, USA, 2012.

42. CSI. *Integrated Software for Structural Analysis and Design*; Computers and Structures Inc.: Berkeley, CA, USA, 2020.

43. Yoo, J.H.; Lehman, D.E.; Roeder, C.W. Influence of connection design parameters on the seismic performance of braced frames. *J. Constr. Steel Res.* **2008**, *64*, 608–622. [CrossRef]

44. Uriz, P.; Filippou, F.C.; Mahin, S.A. Model for cyclic inelastic buckling for steel member. *J. Struct. Eng. ASCE* **2008**, *134*, 619–628. [CrossRef]

45. Wijesundara, K.K.; Bolognini, D.; Nascimbene, R.; Calvi, G.M. Review of design parameters of concentrically braced frames with RHS shape braces. *J. Earthq. Eng.* **2009**, *13*, 109–131. [CrossRef]

46. Jong, W.H. Seismic Analysis and Evaluation of Several Recentering Braced Frame Structures. *Proc. Inst. Mech. Eng. Part C J. Mech. Eng. Sci.* **2013**, *228*, 781–798.

47. Pinho, R. Adaptive and non-adaptive nonlinear static analysis of irregular structures. In Proceedings of the RELUIS Conference on Assessment and Mitigation of Seismic Vulnerability of Existing Reinforced Concrete Structures, Rome, Italy, 23 November 2008.

48. Pinho, R. Using pushover analysis for assessment of buildings and bridges. *CISM Int. Cent. Mech. Sci. Courses Lect.* **2007**, *494*, 91–120.

49. Borzi, B.; Pinho, R.; Crowley, H. Simplified pushover-based vulnerability analysis for large-scale assessment of RC buildings. *Eng. Struct.* **2008**, *30*, 804–820. [CrossRef]

50. Iervolino, I.; Galasso, C.; Cosenza, E. Selezione assistita di input sismico e nuove Norme Tecniche per le Costruzioni. In Proceedings of the RELUIS Conference on Assessment and Mitigation of Seismic Vulnerability of Existing Reinforced Concrete Structures, Rome, Italy, 23 November 2008.